Endoplasmic reticulum stress enhances fibrotic remodeling in the lungs

William E. Lawson[a,b,1,2], Dong-Sheng Cheng[a,1], Amber L. Degryse[a], Harikrishna Tanjore[a], Vasiliy V. Polosukhin[a], Xiaochuan C. Xu[a], Dawn C. Newcomb[a], Brittany R. Jones[a], Juan Roldan[a,c,d], Kirk B. Lane[a], Edward E. Morrisey[e,f,g], Michael F. Beers[e], Fiona E. Yull[h], and Timothy S. Blackwell[a,b,h,i]

[a]Department of Medicine, Division of Allergy, Pulmonary and Critical Care Medicine, and Departments of [i]Cell and Developmental Biology and [h]Cancer Biology, Vanderbilt University School of Medicine, Nashville, TN 37232; [b]Department of Veterans Affairs Medical Center, Nashville, TN 37212; [c]Fundació Institut d'Investigació Germans Trias i Pujol and [d]Servei de Pneumologia, Hospital Santa Caterina, Calle Dr. Castany, 17190 Salt, Spain; and [e]Department of Medicine, Division of Pulmonary and Critical Care Medicine, [f]Department of Cell and Developmental Biology, and [g]Penn Institute for Regenerative Medicine, University of Pennsylvania School of Medicine, Philadelphia, PA 19104

Edited by Michael J. Welsh, Howard Hughes Medical Institute and University of Iowa, Iowa City, IA, and approved May 18, 2011 (received for review May 11, 2011)

Evidence of endoplasmic reticulum (ER) stress has been found in lungs of patients with familial and sporadic idiopathic pulmonary fibrosis. We tested whether ER stress causes or exacerbates lung fibrosis by (*i*) conditional expression of a mutant form of surfactant protein C (L188Q *SFTPC*) found in familial interstitial pneumonia and (*ii*) intratracheal treatment with the protein misfolding agent tunicamycin. We developed transgenic mice expressing L188Q *SFTPC* exclusively in type II alveolar epithelium by using the Tet-On system. Expression of L188Q *SFTPC* induced ER stress, as determined by increased expression of heavy-chain Ig binding protein (BiP) and splicing of X-box binding protein 1 (XBP1) mRNA, but no lung fibrosis was identified in the absence of a second profibrotic stimulus. After intratracheal bleomycin, L188Q *SFTPC*-expressing mice developed exaggerated lung fibrosis and reduced static lung compliance compared with controls. Bleomycin-treated L188Q *SFTPC* mice also demonstrated increased apoptosis of alveolar epithelial cells and greater numbers of fibroblasts in the lungs. With a complementary model, intratracheal tunicamycin treatment failed to induce lung remodeling yet resulted in augmentation of bleomycin-induced fibrosis. These data support the concept that ER stress produces a dysfunctional epithelial cell phenotype that facilitates fibrotic remodeling. ER stress pathways may serve as important therapeutic targets in idiopathic pulmonary fibrosis.

S100A4 | unfolded protein response

Idiopathic pulmonary fibrosis (IPF) is the most common and severe form of idiopathic interstitial pneumonia (IIP). IPF is characterized by dyspnea, decreased exercise tolerance, and progression to respiratory failure as a result of ongoing fibrotic remodeling of the distal lung parenchyma (1). Although the cause of IPF remains unknown, recent cases of familial interstitial pneumonia (FIP) have begun to shed light on potential pathogenic mechanisms. FIP, which represents a small proportion of IIP, is defined as two or more biologically related family members with a diagnosis of IIP (2, 3). In FIP, 85% of biopsy-proven cases have pathology consistent with usual interstitial pneumonia, the pathological equivalent of IPF (2). In 2002, we reported a large FIP family with a heterozygous mutation in the carboxyl-terminal region of surfactant protein C (*SFTPC*) (4). This exon 5 +128 T→A transversion results in substitution of glutamine for leucine at amino acid 188 (L188Q) in the carboxyl-terminal region of the pro-SFTPC precursor protein (pro-SP-C). This region of pro-SP-C is known as the BRICHOS domain, which is essential for protein folding and processing. Mutations in proteins containing BRICHOS domains are linked to several degenerative and proliferative diseases through mechanisms related to altered posttranslational protein processing (5).

In cultured alveolar epithelial cells (AECs), expression of L188Q *SFTPC* results in a precursor protein that cannot be folded properly in the endoplasmic reticulum (ER), leading to ER stress and activation of the unfolded protein response (UPR) (4, 6, 7). We evaluated lung tissue from individuals with FIP who carried the L188Q mutation and found up-regulation of ER stress markers in the alveolar epithelium (6). Subsequently, we studied lung tissue from individuals with FIP and sporadic IPF without mutations in *SFTPC* and noted that ER stress markers were also present in the alveolar epithelium in the same pattern (6), a finding confirmed by other investigators (8). Therefore, it appears that ER stress and UPR activation are common features of the alveolar epithelium in IPF. These findings raise a number of important and unresolved issues, including whether ER stress causes or exacerbates fibrosis, and, if so, how ER stress in the epithelium regulates fibrotic remodeling. To address these issues, we developed a transgenic mouse model by using the Tet-On system in which mutant L188Q *SFTPC* can be inducibly expressed in type II AECs in the adult mouse. In this model, expression of L188Q *SFTPC* in type II AECs resulted in ER stress and UPR activation; however, no fibrosis was seen in the absence of a second profibrotic stimulus. In contrast, enhanced bleomycin-induced lung fibrosis was found in mice expressing L188Q *SFTPC*, as well as in mice treated with the ER stress-inducing agent tunicamycin, in association with increased epithelial cell death and increased fibroblast accumulation. Our data support the idea that dysfunctional type II AECs facilitate lung fibrosis through increased susceptibility to injury, leading to excessive and dysregulated remodeling.

Results

Expression of Mutant L188Q *SFTPC* Induces ER Stress in AECs. We generated an expression construct under control of the $(\text{tet-O})_7$ promoter containing human *SFTPC* (six exons and introns) with an exon 5 +128 T→A substitution and insertion of an 11-aa myc tag in exon 2 that is expressed in the mature peptide. We also created a construct in which the murine *SFTPC* promoter drives the reverse tetracycline transactivator (rtTA), mSFTPC.rtTA. Cotransfection of mSFTPC.rtTA and $(\text{tet-O})_7$–L188Q *SFTPC*-myc led to doxycycline (Dox)-inducible expression of mutant pro-SP-C in A549 cells (Fig. S1*A*). Next, we purified mSFTPC.rtTA and $(\text{tet-O})_7$–L188Q *SFTPC*-myc constructs, as well as a construct expressing a tetracycline-controlled transcriptional silencer (tTS) under the murine *SFTPC* promoter (mSFTPC.tTS) to prevent

Author contributions: W.E.L., D.-S.C., A.L.D., K.B.L., M.F.B., F.E.Y., and T.S.B. designed research; W.E.L., D.-S.C., A.L.D., H.T., V.V.P., X.C.X., D.C.N., B.R.J., J.R., F.E.Y., and T.S.B. performed research; E.E.M. and M.F.B. contributed new reagents/analytic tools; W.E.L., D.-S.C., A.L.D., H.T., V.V.P., X.C.X., D.C.N., B.R.J., J.R., K.B.L., E.E.M., M.F.B., F.E.Y., and T.S.B. analyzed data; and W.E.L., D.-S.C., and T.S.B. wrote the paper.

The authors declare no conflict of interest.

This article is a PNAS Direct Submission.

[1]W.E.L. and D.-S.C. contributed equally to this work.

[2]To whom correspondence should be addressed. E-mail: william.lawson@vanderbilt.edu.

This article contains supporting information online at www.pnas.org/lookup/suppl/doi:10.1073/pnas.1107559108/-/DCSupplemental.

basal leakiness of transgene expression (9) (Fig. S1*B*) and performed simultaneous pronuclear microinjection of the three DNA constructs into fertilized oocytes from C57BL/6J mice. This strategy leads to tandem integration of constructs into a single integration site in the majority of cases (10). We identified 4 founders (of 52 potential founders) that possessed all three constructs (Fig. S2*A*). Transgenic mice developed normally, appeared healthy, and bred well, transmitting all three transgenes to their progeny. Adult mice were given Dox in drinking water, and RNA was isolated from whole-lung tissue. Evaluation by real-time RT-PCR revealed that induction of L188Q *SFTPC* expression did not affect native pro-SP-C mRNA levels and was ~10-fold less than expression of the endogenous gene in the highest expressing founder line (Fig. S2*B*). Furthermore, mutant L188Q *SFTPC* was expressed for up to 6 mo with continuous exposure to Dox (Fig. S2*C*). Immunohistochemistry (IHC) for the myc-tagged transgene demonstrated that mutant L188Q pro-SP-C expression localized exclusively to cells in corners of alveoli, consistent with the site and appearance of type II AECs (Fig. S2 *D–F*). No transgene expression was identified in the absence of Dox treatment.

Formalin-fixed, paraffin-embedded lung tissue sections were immunostained for the ER stress markers heavy-chain Ig binding protein (BiP) and X-box binding protein 1 (XBP1). BiP is a protein chaperone that assists with protein folding and increases dramatically with protein accumulation and ER stress. XBP1 is a potent transactivator of UPR gene expression, regulating a variety of cellular functions (11, 12). After administration of Dox for 1 wk, both BiP and XBP1 were found by IHC to be up-regulated in type II AECs in L188Q *SFTPC* mice (Fig. 1 *A–D*). In addition, BiP protein and mRNA expression was increased in whole-lung tissue samples after Dox treatment (Fig. 1 *E* and *F*). XBP1 is normally expressed as a full-length unspliced mRNA. When protein accumulation induces ER stress, unspliced XBP mRNA undergoes inositol requiring enzyme 1 (IRE1)-dependent splicing, yielding a spliced XBP1 isoform that permits translation of the biologically active XBP1 protein. The ratio of the spliced isoform to total XBP1 mRNA can be used as a marker of the IRE1-mediated ER stress response (13). Dox-treated L188Q *SFTPC* mice had evidence of increased XBP1 splicing in lung tissue, indicative of ER stress (Fig. 1 *G* and *H*). Together, these studies show that transgene expression in L188Q *SFTPC* mice causes ER stress localized to type II AECs.

After Dox treatment for 1 wk, we isolated primary type II AECs to determine trafficking of the myc-tagged mutant pro-SP-C. In type II AECs from L188Q *SFTPC* mice, immunofluorescence for the myc tag colocalized with BiP, which is expressed exclusively in the ER (Fig. 2 *A–C*). In contrast, myc expression did not colocalize with giantin, which is found in the Golgi apparatus (Fig. 2 *D–F*). Thus, it appears that mutant L188Q *SFTPC* is principally localized to the ER with little presence in the Golgi, suggesting that processing of mutant pro-SP-C is impaired. Consistent with this idea, we have been unable to detect mature myc-tagged SP-C in supernatant of primary type II AECs or in the airway of L188Q *SFTPC*-expressing mice. Consistent with studies using whole-lung tissue, type II AECs from mice with L188Q *SFTPC* expression exhibited greater BiP protein and mRNA expression and increased XBP1 splicing compared with type II AECs from WT mice (Fig. 2 *G–J*). In the absence of Dox treatment, expression of BiP and XBP1 splicing in type II AECs from L188Q *SFTPC* mice were similar to WT cells, confirming the inducibility of ER stress in our model.

Expression of Mutant L188Q *SFTPC* Exacerbates Lung Fibrosis. We treated L188Q *SFTPC* mice for up to 6 mo with Dox to determine whether induction of ER stress was sufficient to cause lung remodeling; however, lungs from these mice appeared histologically normal despite persistent transgene expression (Fig. S3). Although L188Q *SFTPC* expression alone did not result in lung fibrosis, we reasoned that a second stimulus might induce greater fibrosis in L188Q *SFTPC* mice as a result of vulnerable type II AECs. Thus, we turned to intratracheal (i.t.) bleomycin,

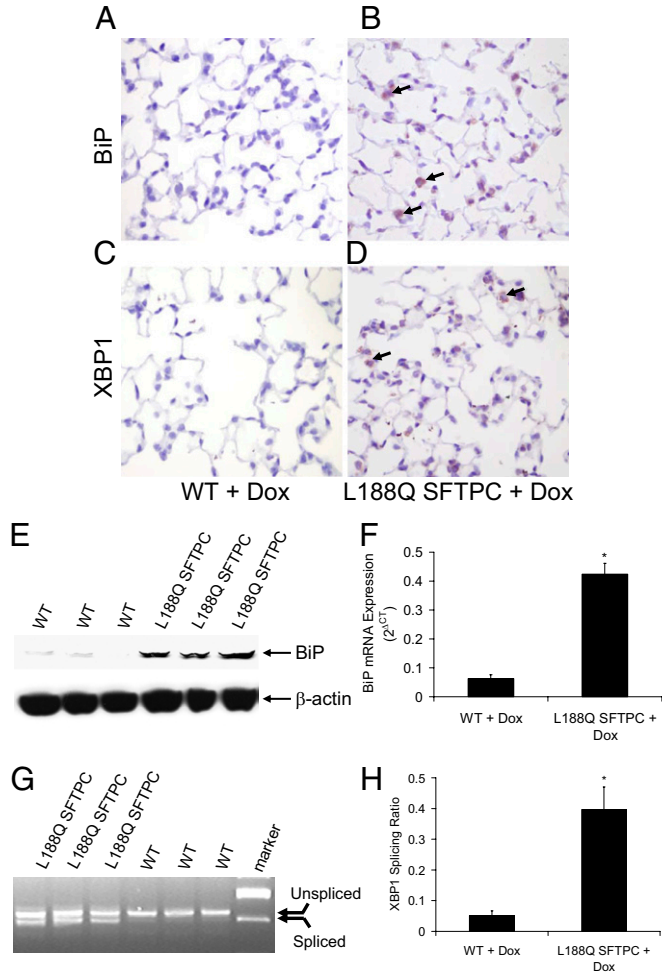

Fig. 1. Expression of mutant L188Q *SFTPC* in vivo leads to ER stress in type II AECs. (*A* and *B*) IHC for BiP in lung sections of WT (*A*) and L188Q *SFTPC* (*B*) mice, both treated with Dox for 1 wk. (*C* and *D*) IHC for XBP1 in lungs from the same mice. (Magnification in *A–D*: ×400.) Arrows point to immunostain-positive cells. (*E*) Western blot analysis on whole-lung lysates for BiP from WT and L188Q *SFTPC* mice treated with Dox for 1 wk. β-Actin is shown as loading control. (*F*) Results of quantitative real-time RT-PCR for expression of BiP mRNA from lungs of mice treated with Dox for 1 wk, normalized to the housekeeping gene RPL19. (n = 4–5 per column; $^*P < 0.001$ between columns.) (*G*) RT-PCR gel demonstrating splice variants for XBP1 mRNA in lungs of L188Q *SFTPC* and WT mice treated with Dox for 1 wk. (*H*) XBP1 splicing analysis by densitometry. (n = 5 per column; $^*P < 0.01$ between columns.) Graphical data are presented as mean ± SEM.

the most commonly used model of experimental lung fibrosis. Mutant L188Q *SFTPC* mice and WT controls were started on Dox and, 1 wk later, received low-dose i.t. bleomycin (0.04 unit); 3 wk later, lung fibrosis was increased in L188Q *SFTPC* mice, as determined by evaluation of trichrome-stained sections (Fig. 3 *A–C*). Furthermore, total lung collagen was greater in L188Q *SFTPC* mice compared with WT mice after bleomycin treatment (Fig. 3*D*). In previous studies, we have used S100A4 as a fibroblast marker in the lungs (14–17). Therefore, we evaluated lung sections by IHC for S100A4 expression and noted greater numbers of S100A4-positive fibroblasts in L188Q *SFTPC* mice compared with WT controls after bleomycin treatment (Fig. S4 *A* and *B* and Fig. 3*E*). Similarly, L188Q *SFTPC* mice had greater numbers of myofibroblasts positive for α-smooth muscle actin (αSMA) in lung parenchyma after bleomycin treatment than WT controls did (Fig. S4 *C* and *D* and Fig. 3*F*).

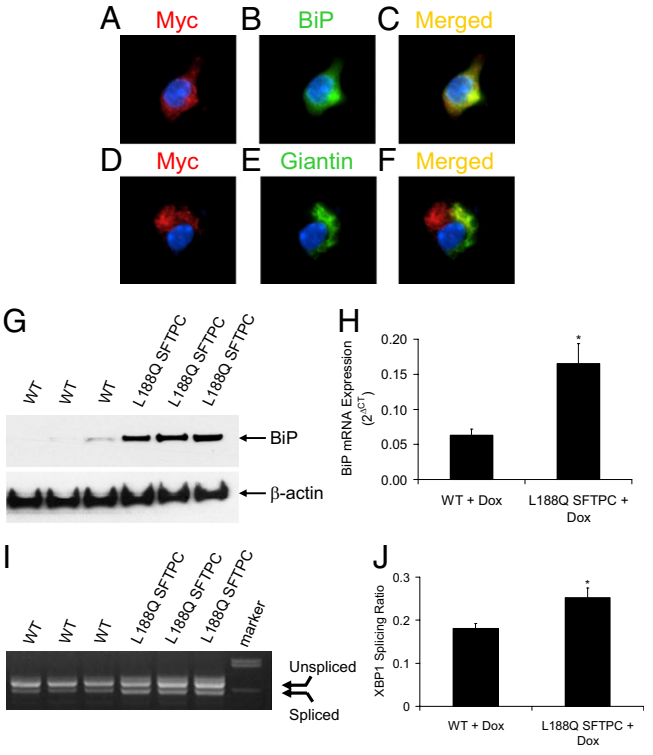

Fig. 2. Mutant L188Q pro-SP-C localizes to the ER in type II AECs isolated from L188Q *SFTPC* mice after in vivo Dox treatment for 1 wk. (*A–C*) Dual immunofluorescence for the myc tag (red; *A*) and the ER marker BiP (green; *B*) demonstrated strong colocalization on merged imaging (yellow; *C*). Blue, DAPI. (*D–F*) Dual immunofluorescence for the myc tag (red; *D*) and the Golgi marker giantin (green; *E*) demonstrated minimal colocalization on merged imaging (yellow; *F*). Blue, DAPI. (G) Western blot analysis for BiP from type II AECs isolated from WT or L188Q *SFTPC* mice treated with Dox in vivo for 1 wk. β-Actin is shown as loading control. (*H*) Real-time RT-PCR for expression of BiP mRNA, normalized to the housekeeping gene RPL19. ($n = 3$ per column; $^*P < 0.05$ between columns.) (*I*) RT-PCR gel demonstrating a splice variant for XBP1 in type II AECs. (*J*) XBP1 splicing analysis by densitometry. ($n = 3$ per column; $^*P < 0.05$ between columns.) Graphical data are presented as mean ± SEM.

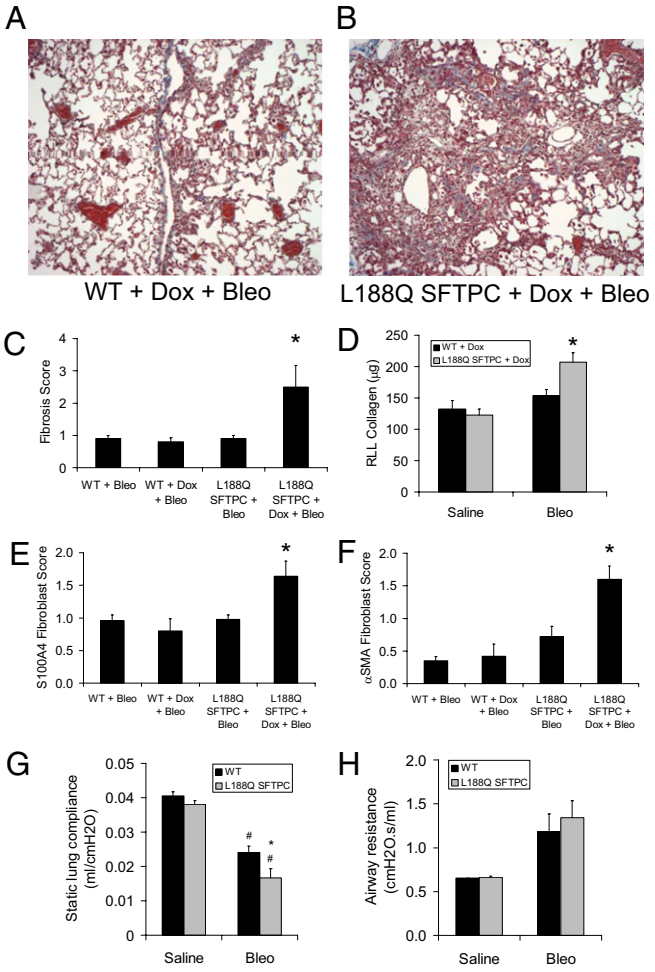

Fig. 3. Mice expressing mutant L188Q *SFTPC* had greater lung fibrosis after i.t. bleomycin (Bleo). (*A* and *B*) Trichrome-stained lung sections from Dox-treated WT mice and L188Q *SFTPC* mice at 3 wk after 0.04 unit of i.t. bleomycin. (Magnification: ×100.) (*C*) Semiquantitative fibrosis scoring of trichrome-stained lung sections from WT and L188Q *SFTPC* mice at 3 wk after 0.04 unit of i.t. bleomycin. ($n = 5$ per group; $^*P < 0.05$ compared with other groups.) Results are representative of three separate experiments. (*D*) Total lung collagen content from right lower lobe (RLL) based on hydroxyproline microplate assay at 3 wk after 0.04 unit of i.t. bleomycin or saline. ($n = 4$–6 per group for saline and 10 per group for bleomycin; $^*P < 0.05$ compared with other groups.) (*E*) Semiquantitative scoring of S100A4+ lung fibroblasts on immunostained lung sections from WT and L188Q *SFTPC* mice at 3 wk after i.t. bleomycin. ($n = 5$ per group; $^*P < 0.05$ compared with other groups.) (*F*) Semiquantitative scoring of αSMA+ lung fibroblasts on immunostained lung sections from WT and L188Q *SFTPC* mice at 3 wk after i.t. bleomycin. ($n = 5$ per group; $^*P < 0.05$ compared with other groups.) (*G*) Static lung compliance in WT and L188Q *SFTPC*-expressing mice treated with Dox at 3 wk after i.t. bleomycin. ($n = 3$ per group for saline and 5–8 per group for bleomycin; $^*P < 0.05$ between bleomycin-treated groups; $^{\#}P < 0.001$ compared with respective saline-treated group.) (*H*) Airway resistance in WT and L188Q *SFTPC*-expressing mice treated with Dox at 3 wk after i.t. bleomycin. Graphical data are presented as mean ± SEM.

Additionally, we wanted to determine whether lung mechanics were different at 3 wk after bleomycin treatment in L188Q *SFTPC* mice. We found that static lung compliance was decreased in both WT mice and L188Q *SFTPC* mice treated with bleomycin compared with their respective saline-treated controls. In the bleomycin-treated group, static lung compliance was further reduced in L188Q *SFTPC* mice compared with WT controls (Fig. 3*G*). No differences were noted in static lung compliance between the two groups in the absence of bleomycin.

Although our findings indicated a profibrotic effect of L188Q *SFTPC* expression, we wondered whether the impact of transgene expression was limited by the relatively low ratio of mutant *SFTPC* expression compared with the endogenous gene. Thus, we crossed L188Q *SFTPC* mice with mice that use the human *SFTPC* promoter (hSFTPC.rtTA) (18), in hopes of increasing mutant L188Q pro-SP-C expression. Dox-inducible mRNA expression of mutant pro-SP-C did increase approximately threefold (Fig. S5*A*), but the mice did not develop spontaneous fibrosis, and lung fibrosis after bleomycin treatment was not different between mutant L188Q *SFTPC* mice with or without hSFTPC.rtTA (Fig. S5*B*). These studies suggest that level of transgene expression is not a limiting factor in determining the phenotype of L188Q *SFTPC*-expressing mice.

Expression of L188Q *SFTPC* Increases AEC Apoptosis After Bleomycin Treatment. Because high levels of ER stress have been linked to increased epithelial cell apoptosis (6, 7, 19), we wanted to determine whether ER stress in L188Q *SFTPC* mice was associated with increased AEC apoptosis. In the absence of bleomycin, TUNEL+ AECs were rare in Dox-treated L188Q *SFTPC* mice and were present in similar numbers compared with WT littermates. We have previously shown that the number of TUNEL+ epithelial cells peaks in the lungs at 1 wk after i.t. bleomycin injection (17). At this time point, lung sections from L188Q *SFTPC* mice showed greater numbers of TUNEL+ AECs than lungs from WT controls did (Fig. 4 *A–C*), indicative of greater AEC apoptosis. This finding indicates that AECs in L188Q *SFTPC*

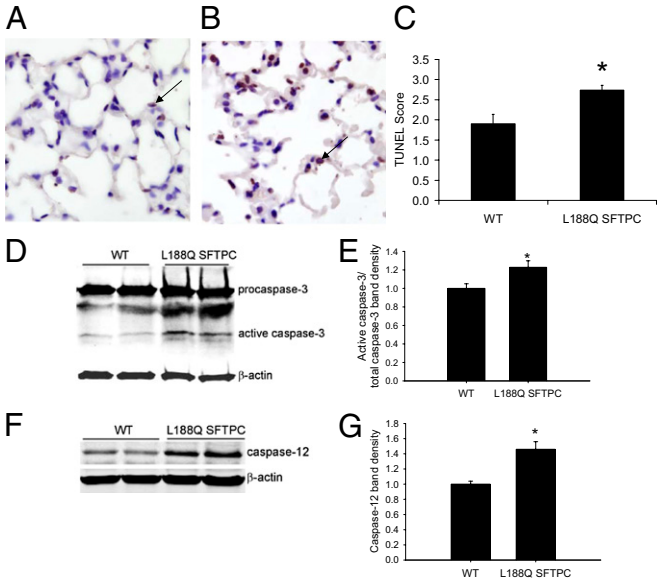

Fig. 4. Mice expressing L188Q *SPTPC* had greater AEC death after i.t. bleomycin. (*A* and *B*) TUNEL-stained lung sections from WT (*A*) and L188Q *SFTPC* (*B*) mice at 1 wk after i.t. bleomycin. Arrows point to representative TUNEL+ cells. (Magnification: ×600.) (*C*) Semiquantitative evaluation of TUNEL+ AECs on lung sections from WT and L188Q *SFTPC* mice at 1 wk after i.t. bleomycin. (n = 8–11 per group; *$P < 0.05$ between groups.) (*D* and *E*) Western blot analysis (*D*) and densitometry (*E*) for caspase-3 using whole-lung lysates from bleomycin-treated WT and L188Q *SFTPC* mice. β-Actin was used as a loading control. Graphical data represent the ratio of band densities for active caspase-3 and total caspase-3 (WT normalized to value of 1). (n = 5 per group; *$P < 0.05$ compared with WT.) (*F* and *G*) Western blot analysis (*F*) and densitometry (*G*) for caspase-12 from lung lysates. Graphical data represent the band density of caspase-12 adjusted for β-actin (WT normalized to value of 1). (n = 5 per group; *$P < 0.05$ compared with WT.) Graphical data are presented as mean ± SEM.

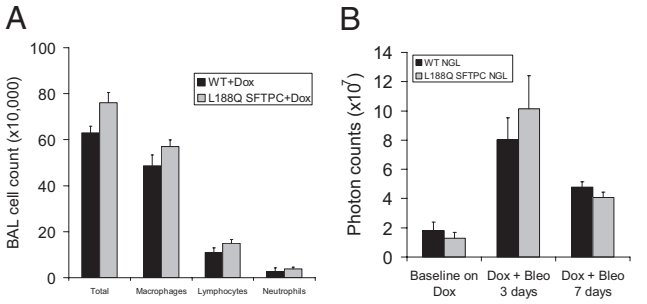

Fig. 5. Mutant L188Q *SFTPC* expression does not enhance lung inflammation after i.t. bleomycin (Bleo). (*A*) Total and differential cell counts in bronchoalveolar lavage (BAL) from WT and L188Q *SFTPC* mice at 1 wk after i.t. bleomycin. (n = 5–6 per group). (*B*) Bioluminescence imaging over the thorax as an indicator of NF-κB activation in lungs of WT and L188Q *SFTPC* mice crossed with NGL mice. Baseline photon counts represent mice with Dox treatment for 14 d. Subsequently, mice were treated with bleomycin and imaged at 3 and 7 d. Photon counting was performed after i.p. injection of luciferin (1 mg). (n= 4 per group.) Graphical data are presented as mean ± SEM.

mice are more susceptible to bleomycin-induced injury. Furthermore, active caspase-3 expression was increased in the lungs of L188Q *SFTPC* mice compared with WT controls (Fig. 4 *D* and *E*), suggesting that caspase-dependent cell-death pathways are selectively activated in the presence of ER stress in this model. ER stress has been linked to apoptosis through activation of ER-bound caspase-12 in mice (caspase-4 in humans) (20, 21). By Western blot analysis from whole-lung lysates, we noted that caspase-12 expression was increased in L188Q *SFTPC* mice at 1 wk after bleomycin treatment compared with WT controls (Fig. 4 *F* and *G*). Apoptosis mediated through expression of CCAAT/enhancer-binding protein homologous transcription factor (CHOP) has also been linked to ER stress (22), but we did not identify increased CHOP expression in our model.

Interestingly, we found that BiP mRNA expression and XBP1 splicing were increased in lungs of WT mice at 1 wk after bleomycin treatment (Fig. S6). In addition, BiP expression was further increased in the lungs of L188Q *SFTPC* mice treated with bleomycin in addition to Dox, although XBP1 splicing was unchanged. Together, these findings indicate that bleomycin itself induces ER stress in the lungs, potentially contributing to the pathological lung remodeling in this model.

Next, we asked whether L188Q *SFTPC* mice had altered lung inflammation after bleomycin. At 1 wk after bleomycin treatment, L188Q *SFTPC* and WT mice had similar total cells, neutrophils, macrophages, and lymphocytes in bronchoalveolar lavage (Fig. 5*A*). To further evaluate inflammatory signaling in the lungs, we crossed L188Q *SFTPC* mice to NF-κB/GFP/luciferase (NGL) reporter mice. The NGL reporter mouse expresses luciferase as a function of NF-κB activation, providing a surrogate readout of inflammatory pathway activation (23). With Dox alone, neither WT/NGL nor L188Q *SFTPC*/NGL mice had increased luciferase expression above baseline, and values were similar between the two groups. After bleomycin treatment, luciferase expression increased similarly in both groups (Fig. 5*B* and Fig. S7). Furthermore, whole-lung luciferase levels were similar between WT/NGL and L188Q *SFTPC*/NGL mice after 14 d of Dox alone (23.4 ± 22.5 vs. 22.5 ± 11.7 relative light units per μg/μL) and after 14 d of Dox + bleomycin (285.7 ± 53.4 vs. 297.3 ± 58.7 relative light units per μg/μL). Thus, we found no evidence for differences in bleomycin-induced inflammation in L188Q *SFTPC*-expressing mice.

Induction of ER Stress via Tunicamycin Administration Enhances Bleomycin-Induced Lung Fibrosis. Although our data suggest that ER stress is the underlying process by which L188Q *SFTPC* expression contributes to lung fibrosis, we sought to determine whether ER stress induced by other means could lead to a similar phenotype. Among ER stress-inducing agents, tunicamycin, an antibiotic that induces ER stress by blocking *N*-linked protein glycosylation, is the most commonly used (24). We administered i.t. tunicamycin (20 μg/mL in 100 μL of 20% DMSO diluted in PBS) to WT (C57BL/6J background) mice. IHC on sections of lungs harvested 2 d later showed that BiP and XBP1 were induced most prominently in AECs after tunicamycin treatment (Fig. S8 *A–D*). Tunicamycin also induced BiP protein and mRNA expression and XBP1 mRNA splicing in whole-lung samples (Fig. S8 *E–H*). As with L188Q *SFTPC* expression, there was no evidence of lung fibrosis or architectural change 3 wk after a single dose of tunicamycin or after twice-weekly tunicamycin administration for 3 wk. We then tested the combination of tunicamycin followed by bleomycin treatment. WT mice received i.t. tunicamycin (or vehicle control) followed 48 h later by i.t. bleomycin (0.04 unit). At 2 wk after bleomycin injection, the tunicamycin + bleomycin group had much greater lung fibrosis than the vehicle + bleomycin group (Fig. 6 *A–D*). Thus, tunicamycin-induced ER stress resulted in a similar profibrotic phenotype as in the L188Q *SFTPC* model, strongly supporting the idea that ER stress facilitates lung fibrosis.

Discussion

Evaluation of IPF lung biopsies reveals evidence of ER stress in AECs lining the areas of fibrosis (6, 8), but the degree to which ER stress contributes to disease pathogenesis remains undefined. Although *SFTPC* mutation-associated interstitial lung disease is rare in the broad scope of IPF (25), modeling such mutations may serve as a paradigm to better understand IPF and the role of ER stress. With these studies, we have shown that expression of mutant L188Q *SFTPC* results in ER stress in type II AECs in vivo, leading to a vulnerable type II AEC population that is highly susceptible to the effects of bleomycin. With expression of L188Q *SFTPC* and resultant ER stress, AECs were more prone

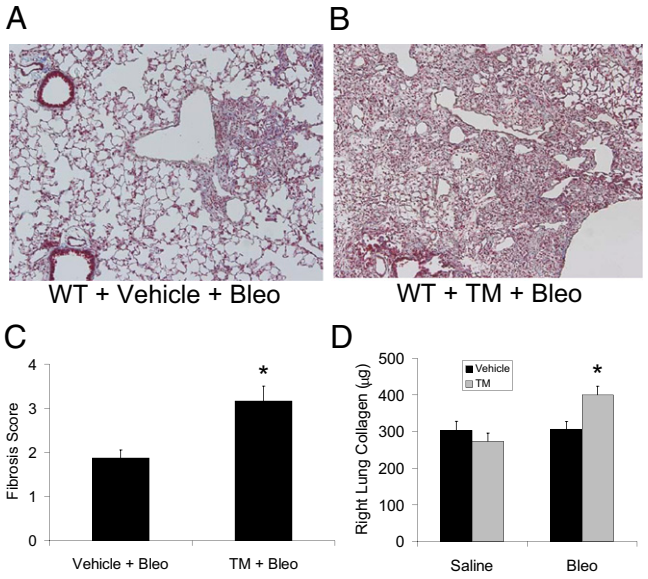

Fig. 6. Tunicamycin (TM) enhances lung fibrosis induced by bleomycin (Bleo). (*A* and *B*) Trichrome-stained lung sections at 2 wk after bleomycin from WT mice treated with a single i.t. injection of vehicle (DMSO; *A*) or tunicamycin (*B*) at 48 h before bleomycin. (Magnification: ×100.) (*C*) Semiquantitative fibrosis scoring of trichrome-stained lung sections from mice exposed to vehicle + bleomycin (vehicle + Bleo) compared with tunicamycin + bleomycin (TM + Bleo) at 2 wk after i.t. bleomycin. (n = 5–6 per group; $^*P < 0.05$ between groups.) (*D*) Total collagen content of entire right lung from mice exposed to vehicle or tunicamycin followed by i.t. administration of saline or bleomycin. (n = 5 per group for saline and 7–10 per group for bleomycin; $^*P < 0.05$ compared with other groups.) Graphical data are presented as mean ± SEM.

to apoptosis after bleomycin treatment, and greater numbers of lung fibroblasts were observed, findings that could explain enhanced fibrosis in the mutant L188Q *SFTPC* mice. In addition, the fact that a similar phenotype was observed when tunicamycin was administered provides a confirmatory model that ER stress in the alveolar epithelium predisposes this cell population to greater injury, driving enhanced fibrosis.

Multiple cases of pediatric and adult interstitial lung disease have been linked to *SFTPC* mutations (4, 25–29), including reports of a mutation that deletes exon 4 and its 37 aa ($SFTPC^{\Delta exon4}$ mutation) (26) and the L188Q mutation analyzed here (4). Both mutations have been analyzed in vitro, revealing that expression of these mutant pro-SP-C forms results in protein accumulation in the ER, ER stress, UPR activation, and increased apoptosis through activation of ER-associated caspase-12/4 (6, 7, 19). In the first evaluation of an *SFTPC* mutation in vivo, Bridges et al. designed a transgenic mouse expressing mutant $SFTPC^{\Delta exon4}$ under the human *SFTPC* promoter, which was expressed during embryogenesis and resulted in ER stress and in utero lethality (30). Although transgene expression in our model was restricted to adulthood and bypassed the issue of effects on lung development, it is likely that the $SFTPC^{\Delta exon4}$ mutation is more severe than the L188Q mutation because patients with this mutation exclusively present with interstitial lung disease in early childhood.

With protein accumulation in the ER, UPR pathways are activated in an attempt to control ER stress and protect the cell (11). The UPR has three main pathways governed by three ER transmembrane proteins: IRE1, activating transcription factor 6 (ATF6), and PKR-like ER kinase (PERK) (11). In the absence of ER stress, these sensors are maintained in their inactive state because of binding by BiP. With ER stress, BiP is released to serve as a folding chaperone, allowing activation of each sensor (31). IRE1 activation allows its intrinsic endonuclease activity to splice XBP1 to its active state, leading to expression of UPR-mediated protein degradation enzymes such as ER degradation-enhancing α-mannosidase–like protein (EDEM) and chaperone proteins (12). ATF6 activation leads to up-regulation of protein-folding chaperone proteins such as BiP (32) and to the increased expression of XBP1 (12). Activation of PERK leads to a phosphorylated eukaryotic initiation factor 2α (p-eIF2α)–dependent global attenuation of protein translation and an ATF4-dependent expression of redox and metabolism proteins (33). Together, these three UPR pathways are designed to attenuate ER stress. However, with severe or prolonged ER stress, UPR mechanisms can lead to activation of apoptosis pathways (11). ER stress can trigger apoptosis by induction of CHOP/GADD153, via activation of caspase-12/4, and through phosphorylation of eIF2α. In our studies with L188Q *SFTPC* mice and in humans with IPF (6), we have not identified increased p-eIF2α. In addition, we did not find up-regulation of CHOP. We did, however, note increased caspase-12 levels in the lung after bleomycin treatment in mutant L188Q *SFTPC* mice compared with littermate controls. ER-bound caspase-12 (and its human homolog, casapse-4) has been linked to ER stress-induced apoptosis (20, 21). Previous studies by Mulugeta et al. detailed that mutant forms of *SFTPC*, including L188Q, lead to caspase-4–mediated caspase-3 activation and cell apoptosis in vitro (7), a finding complementary to results from our in vivo model. AEC apoptosis has been linked to fibrosis in both human IPF lung biopsy samples (34) and in animal models (35), including in a recent study by Sisson et al. in which directed expression of diphtheria toxin by means of the *SFTPC* promoter led to type II AEC apoptosis and lung fibrosis (36). Thus, increased apoptosis may be one of the mechanisms contributing to exuberant fibrosis in L188Q *SFTPC* mice.

In our models, expression of L188Q *SFTPC* and treatment with tunicamycin induce ER stress but do not result in fibrotic remodeling, suggesting that murine type II AECs are able to manage the UPR response without obvious pathology. Rather, ER stress likely places the type II AEC population in a vulnerable state in which a second stimulus, in this case bleomycin, exerts a prominent effect, leading to enhanced lung fibrosis. Given the fact that patients with FIP, including many with *SFTPC* mutations, frequently present with interstitial lung disease in adulthood, one could infer that a "second hit" might be required to induce clinical disease in at-risk individuals. In FIP (and sporadic IPF), the relevant injurious stimulus likely results from an environmental exposure, but the nature of this agent(s) is currently unknown. To date, only a history of cigarette smoking and the presence of herpesvirus antigens in the lungs have been associated with clinical disease in FIP. Hopefully, future studies with L188Q *SFTPC*-expressing mice or other genetic models treated with relevant environmental stimuli will help clarify the potential second hits that contribute to lung fibrosis.

In summary, our studies demonstrate that ER stress in AECs predisposes the lung to greater injury and fibrosis in experimental models. These findings provide mechanistic information supporting an important role for ER stress, which is prominent in the lungs of individuals with IPF, in disease pathogenesis. ER stress and downstream UPR pathways may serve as therapeutic targets for future interventions in this devastating lung disease.

Materials and Methods

Transgenic Mice. To generate transgenic mutant L188Q *SFTPC* mice, three constructs were coinjected at the Vanderbilt Transgenic/ES Shared Resource facility (Fig. S1): (*i*) $(tet\text{-}O)_7$–L188Q *SFTPC*-myc, (*ii*) mSFTPC.rtTA, and (*iii*) mSFTPC.tTS (37). Transgenic mice expressing rtTA under the human SFTPC promoter (hSFTPC.rtTA) were obtained from Jackson Laboratories. NGL mice, which have consensus NF-κB binding sites upstream of the HSV minimal thymidine kinase promoter driving the GFP/luciferase construct, have been described previously (23). All mice were C57BL/6J background and entered experiments at 8–10 wk of age. All mouse experiments were approved by the Vanderbilt Institutional Animal Care and Use Committee.

Animal Model and Drug Administration. Bleomycin (0.04 unit) (Bedford Laboratories) was injected i.t. in mice by intubation as previously described (17). Lungs were harvested for histology, frozen tissue, bronchoalveolar lavage,

or cell isolation as previously described (14–17). L188Q *SFTPC* mice and controls were maintained on normal water ad libitum until transgene activation was desired. Then, mice were given Dox (Sigma-Aldrich) in sterile water (2 g/dL with additional 2% sucrose).

Tunicamycin (Sigma) was dissolved in DMSO and diluted to 20 μg/mL in 20% DMSO diluted in PBS, and then 100 μL of solution was delivered to mice by i.t. intubation. A similar volume of 20% DMSO diluted in PBS was used as vehicle control.

Lung Sample Processing and Analysis. Formalin-fixed lung sections were prepared as previously described (14–16). IHC (14, 15), immunofluorescence (16, 17), TUNEL (15, 17), and bronchoalveolar lavage with cell counts (15, 17) were performed as previously described. RNA isolation, real-time RT-PCR, and Western blot analysis were performed by using standard techniques (detailed in *SI Materials and Methods*).

Cell Culture/Isolation. Plasmids were transfected into A549 cells with an Effectene transfection kit (Qiagen) per the manufacturer's instructions. Cells were incubated with the transfection complexes under normal growth conditions for 4 h, and then 0.5–1.0 μg/mL Dox was added to the medium. After 24 h, cells were harvested for Western blot analysis. Type II AECs were isolated as previously described (14, 16).

In Vivo Bioluminescence and Luciferase Measurements. Live bioluminescence imaging was performed after i.p. injection of luciferin (1 mg in 100 μL of saline), and whole-lung tissue luciferase levels were determined as previously described (23).

Measurement of Airway Resistance and Compliance. For airway resistance and compliance measurements, mice were anesthetized with i.p. pentobarbital, and tracheas were cannulated with a 20-gauge metal stub adapter. Each mouse was placed on a small-animal ventilator, flexiVent (SCIREQ), with 150 breaths per min and a tidal volume of 10 mL/kg of body weight. Airway resistance (cm of H_2O/mL per s) and static lung compliance (using a 2-s breath pause) (mL/cm of H_2O) were determined with the manufacturer's software.

Semiquantitative Scoring and Collagen Content. Scoring of lung fibrosis (15, 17), fibroblasts (15), and TUNEL staining (9) and determination of collagen content by hydroxyproline assay (38) were performed as previously described.

Statistics. Statistical analyses were performed with InStat (GraphPad Software). Differences among groups were assessed with one-way ANOVA and between pairs with Student's *t* test. Results are presented as mean ± SEM. *P* values <0.05 were considered significant.

Detailed methods are available in *SI Materials and Methods*.

ACKNOWLEDGMENTS. We thank Linda A. Gleaves and Frank B. McMahon for work in our histology core laboratory and the Vanderbilt Transgenic/ES Shared Resource facility for assistance with generation of the L188Q *SFTPC* mice.

1. American Thoracic Society European Respiratory Society (2000) Idiopathic pulmonary fibrosis: Diagnosis and treatment. International consensus statement. *Am J Respir Crit Care Med* 161:646–664.
2. Steele MP, et al. (2005) Clinical and pathologic features of familial interstitial pneumonia. *Am J Respir Crit Care Med* 172:1146–1152.
3. Lawson WE, Loyd JE (2006) The genetic approach in pulmonary fibrosis: Can it provide clues to this complex disease? *Proc Am Thorac Soc* 3:345–349.
4. Thomas AQ, et al. (2002) Heterozygosity for a surfactant protein C gene mutation associated with usual interstitial pneumonitis and cellular nonspecific interstitial pneumonitis in one kindred. *Am J Respir Crit Care Med* 165:1322–1328.
5. Beers MF, Mulugeta S (2005) Surfactant protein C biosynthesis and its emerging role in conformational lung disease. *Annu Rev Physiol* 67:663–696.
6. Lawson WE, et al. (2008) Endoplasmic reticulum stress in alveolar epithelial cells is prominent in IPF: Association with altered surfactant protein processing and herpesvirus infection. *Am J Physiol Lung Cell Mol Physiol* 294:L1119–L1126.
7. Mulugeta S, et al. (2007) Misfolded BRICHOS SP-C mutant proteins induce apoptosis via caspase-4- and cytochrome *c*-related mechanisms. *Am J Physiol Lung Cell Mol Physiol* 293:L720–L729.
8. Korfei M, et al. (2008) Epithelial endoplasmic reticulum stress and apoptosis in sporadic idiopathic pulmonary fibrosis. *Am J Respir Crit Care Med* 178:838–846.
9. Cheng DS, et al. (2007) Airway epithelium controls lung inflammation and injury through the NF-&kappaB pathway. *J Immunol* 178:6504–6513.
10. Lee CG, et al. (2004) Early growth response gene 1-mediated apoptosis is essential for transforming growth factor &beta1-induced pulmonary fibrosis. *J Exp Med* 200:377–389.
11. Schröder M, Kaufman RJ (2005) The mammalian unfolded protein response. *Annu Rev Biochem* 74:739–789.
12. Yoshida H, Matsui T, Yamamoto A, Okada T, Mori K (2001) XBP1 mRNA is induced by ATF6 and spliced by IRE1 in response to ER stress to produce a highly active transcription factor. *Cell* 107:881–891.
13. Shang J (2005) Quantitative measurement of events in the mammalian unfolded protein response. *Methods* 35:390–394.
14. Lawson WE, et al. (2005) Characterization of fibroblast-specific protein 1 in pulmonary fibrosis. *Am J Respir Crit Care Med* 171:899–907.
15. Lawson WE, et al. (2005) Increased and prolonged pulmonary fibrosis in surfactant protein C-deficient mice following intratracheal bleomycin. *Am J Pathol* 167: 1267–1277.
16. Tanjore H, et al. (2009) Contribution of epithelial-derived fibroblasts to bleomycin-induced lung fibrosis. *Am J Respir Crit Care Med* 180:657–665.
17. Degryse AL, et al. (2010) Repetitive intratracheal bleomycin models several features of idiopathic pulmonary fibrosis. *Am J Physiol Lung Cell Mol Physiol* 299:L442–L452.
18. Perl AK, Wert SE, Nagy A, Lobe CG, Whitsett JA (2002) Early restriction of peripheral and proximal cell lineages during formation of the lung. *Proc Natl Acad Sci USA* 99: 10482–10487.
19. Mulugeta S, Nguyen V, Russo SJ, Muniswamy M, Beers MF (2005) A surfactant protein C precursor protein BRICHOS domain mutation causes endoplasmic reticulum stress, proteasome dysfunction, and caspase 3 activation. *Am J Respir Cell Mol Biol* 32: 521–530.
20. Hitomi J, et al. (2004) Involvement of caspase-4 in endoplasmic reticulum stress-induced apoptosis and Aβ-induced cell death. *J Cell Biol* 165:347–356.
21. Hitomi J, et al. (2004) Apoptosis induced by endoplasmic reticulum stress depends on activation of caspase-3 via caspase-12. *Neurosci Lett* 357:127–130.
22. Ma Y, Brewer JW, Diehl JA, Hendershot LM (2002) Two distinct stress signaling pathways converge upon the CHOP promoter during the mammalian unfolded protein response. *J Mol Biol* 318:1351–1365.
23. Everhart MB, et al. (2006) Duration and intensity of NF-&kappaB activity determine the severity of endotoxin-induced acute lung injury. *J Immunol* 176:4995–5005.
24. Reimertz C, Kögel D, Rami A, Chittenden T, Prehn JH (2003) Gene expression during ER stress-induced apoptosis in neurons: Induction of the BH3-only protein Bbc3/PUMA and activation of the mitochondrial apoptosis pathway. *J Cell Biol* 162:587–597.
25. Lawson WE, et al. (2004) Genetic mutations in surfactant protein C are a rare cause of sporadic cases of IPF. *Thorax* 59:977–980.
26. Nogee LM, et al. (2001) A mutation in the surfactant protein C gene associated with familial interstitial lung disease. *N Engl J Med* 344:573–579.
27. Crossno PF, et al. (2010) Identification of early interstitial lung disease in an individual with genetic variations in *ABCA3* and *SFTPC*. *Chest* 137:969–973.
28. van Moorsel CH, et al. (2010) Surfactant protein C mutations are the basis of a significant portion of adult familial pulmonary fibrosis in a Dutch cohort. *Am J Respir Crit Care Med* 182:1419–1425.
29. Nogee LM, et al. (2002) Mutations in the surfactant protein C gene associated with interstitial lung disease. *Chest* 121(3, Suppl):20S–21S.
30. Bridges JP, Wert SE, Nogee LM, Weaver TE (2003) Expression of a human surfactant protein C mutation associated with interstitial lung disease disrupts lung development in transgenic mice. *J Biol Chem* 278:52739–52746.
31. Bertolotti A, Zhang Y, Hendershot LM, Harding HP, Ron D (2000) Dynamic interaction of BiP and ER stress transducers in the unfolded-protein response. *Nat Cell Biol* 2: 326–332.
32. Wang Y, et al. (2000) Activation of ATF6 and an ATF6 DNA binding site by the endoplasmic reticulum stress response. *J Biol Chem* 275:27013–27020.
33. Harding HP, Zhang Y, Bertolotti A, Zeng H, Ron D (2000) *Perk* is essential for translational regulation and cell survival during the unfolded protein response. *Mol Cell* 5:897–904.
34. Uhal BD, et al. (1998) Alveolar epithelial cell death adjacent to underlying myofibroblasts in advanced fibrotic human lung. *Am J Physiol* 275:L1192–L1199.
35. Hagimoto N, Kuwano K, Nomoto Y, Kunitake R, Hara N (1997) Apoptosis and expression of Fas/Fas ligand mRNA in bleomycin-induced pulmonary fibrosis in mice. *Am J Respir Cell Mol Biol* 16:91–101.
36. Sisson TH, et al. (2010) Targeted injury of type II alveolar epithelial cells induces pulmonary fibrosis. *Am J Respir Crit Care Med* 181:254–263.
37. Zhu Z, Ma B, Homer RJ, Zheng T, Elias JA (2001) Use of the tetracycline-controlled transcriptional silencer (tTS) to eliminate transgene leak in inducible overexpression transgenic mice. *J Biol Chem* 276:25222–25229.
38. Brown S, Worsfold M, Sharp C (2001) Microplate assay for the measurement of hydroxyproline in acid-hydrolyzed tissue samples. *Biotechniques* 30:38–40, 42.